Int. J. Electrochem. Sci., 15 **(2020)** 5597 – 5608, doi: 10.20964/2020.06.81

International Journal of
ELECTROCHEMICAL
SCIENCE
www.electrochemsci.org

Tuning the Activity and Stability of Platinum Nanoparticles Toward the Catalysis of the Formic Acid Electrooxidation

Islam M. Al-Akraa[1], Bilquis Ali Al-Qodami[2], Mysore Sridhar Santosh[3], R. Viswanatha[4], Abdul Kareem Thottoli[5], Ahmad M. Mohammad[2,]*

[1] Department of Chemical Engineering, Faculty of Engineering, The British University in Egypt, Cairo 11837, Egypt
[2] Chemistry Department, Faculty of Science, Cairo University, Cairo 12613, Egypt
[3]Center for Incubation, Innovation, Research and Consultancy (CIIRC), Jyothy Institute of Technology, Thataguni, Off Kanakapura Road, Bangalore -560082, Karnataka, India
[4]Department of Chemistry, Jyothy Institute of Technology, Thataguni, Off Kanakapura Road, Bangalore - 560082, Karnataka, India
[5]Department of Physics, PSMO College, Tirurangadi, Malappuram, Kerala 676306, India
[*]E-mail: ammohammad@cu.edu.eg

Received: 18 January 2020 / *Accepted:* 4 April 2020 / *Published:* 10 May 2020

The impact of tuning the electrodeposition potential (E_{Pt})of platinum nanoparticles (PtNPs) on the catalytic activity and stability of PtNPs–modified glassy carbon (GC) (Pt/GC) catalysts toward the formic acid electro–oxidation (FAO) was electrochemically examined. Practically, different potentials (E_{Pt}= – 0.20, – 0.10, 0.00, 0.10 and 0.20 V) comprising the underpotential and overpotential deposition domains of PtNPs were employed while passing the same coulombic charge (10 mC) which ensured the deposition of the same loadings of PtNPs. The investigation disclosed the critical role of the deposition potential of PtNPs in the Pt/GC catalyst on justifying not only the catalyst's activity toward FAO which appeared boosted largely at the border potentials (E_{Pt}= – 0.20 and 0.20 V) but also the catalyst's stability which owned the highest durability at 0 V. Several indices utilizing the current densities of the direct (favorable dehydrogenation) oxidation peak (I_p^d), the indirect (unfavorable dehydration – poisoning) oxidation peak (I_p^{ind}) and the backward oxidation peak (I_p^b) in the cyclic voltammetry of FAO were utilized to assess and compare the catalytic efficiencies of the catalysts. Interestingly, for the Pt/GC catalyst (E_{Pt}= 0.2 V), the I_p^d/I_p^{ind} ratio was 8 which reflected the preference of the FAO's mechanism to proceed via the favorable dehydrogenation pathway, while the I_p^d/I_p^b ratio was 0.77 which, moreover, highlighted the high tolerance of the catalyst for CO poisoning. While the catalytic enhancement of FAO was predominantly electronic at – 0.20 V, it presumably originated geometrically at 0.20 V; as revealed from the electrochemical impedance spectroscopy.

Keywords: Formic acid electro–oxidation; Pt nanoparticles; Electrodeposition potential; Fuel cells.

1. INTRODUCTION

The rapid increase in the population and the harmful environmental consequences with the rapid depletion of fossil fuels motivated a global consciousness to explore alternative clean abundant power sources [1-9]. Referring to their unique efficiencies, reliability, robustness, green nature and moving flexibility, the proton exchange membrane fuel cells (PEMFCs) represented a convenient replacement to transport the power generators rather than to transmit electricity which is generally produced from fossil fuels [10-15]. One of the key challenges that turns the movement of PEMFCs into a real marketing difficult relates to the fuel's selection. In this regard, the fuel's phase, purity, security of supply, carbon content, water content, availability, cost, toxicity, calorific value, gravimetric and volumetric density and finally compatibility in fuel cells (FCs) have to be competitively assessed.

While H_2 "the smallest carbon-free fuel" remained for long time the headmost for PEMFCs applications, its gaseous nature, low energy density, high cost of miniaturizing its pressurized tanks and critical hazardous associating its carriage, storage and use steered research to small "low-carbon-content" liquid fuels as formic acid (FA). In reality, FA is a safe "non-explosive" and efficient fuel of a high volumetric energy density (1750 kWh L^{-1}). It also exhibited a much lower crossover through Nafion membranes (the typical electrolytes in PEMFCs) than many other liquid fuels as methanol and ethylene glycol; a feature presaging the release of highly compact FCs of ultra-thin membranes [16-18]. Additionally, the direct formic acid FCs (DFAFCs) enjoyed a higher thermodynamic open-circuit potential (1.4 V vs. RHE) than the H_2/O_2 FCs (1.23 V vs. RHE) [19, 20], which consequently, called for intensifying the fundamental research on the catalysis of FA electro−oxidation (FAO); the principal anodic reaction in the DFAFCs [3, 4, 21-25]. Nevertheless, the DFAFCs experience, unfortunately, a gradual dissipation in their performance due to poisoning of the Pt catalyst that was typically employed for FAO. This generally occurs because of the strong adsorption of CO (is generated easily from the “non-faradaic” dissociation of FA) on the Pt surface [26-29]. To admit the DFAFCs strongly into a real marketing, the CO poisoning of the Pt catalyst has to be overcome.

With the advanced revolution in nanoscience, novel nano-sized materials have shown unique characteristics for electronic, water disinfection, electrocatalysis and power applications [30-33]. For instance, transition metal/metal oxide nanostructures have potential applications as catalytic mediators in electrocatalysis [8, 9, 34-36]. In DFAFCs, the modification of Pt surface with transition metal/metal oxide nanostructures represented a successful avenue to overcome the catalyst's poisoning and to enhance the overall cell performance [25, 37-39]. This amendment appeared much better than to switch into Pd-based catalysts which might show a higher efficiency for FAO than Pt but with a much lower durability [40-43].

For long time ago, the Pt catalyst was typically deposited in the form of small nanoparticles (PtNPs) of an average particle size of ca. 65 nm by potential step electrolysis from 1 to 0.1 V vs. Ag/AgCl/KCl (sat.) electrode [24]. The catalytic efficiency of this Pt/GC catalyst was probed from the I_p^d/I_p^{ind} and the I_p^d/I_p^b ratios which read 0.45 and 0.29, respectively. While varying the layer-by-layer "sequential" to the simultaneous "co-deposition" modes of amending the Pt catalysts with transition metal/metal oxides, we observed a large increase in the I_p^d/I_p^{ind} (0.76) and the I_p^d/I_p^b (0.39) ratios when PtNPs were deposited potentiostatically at −0.2 V vs. saturated calomel electrode [21, 22]. This

motivated us to investigate the effect of E_{Pt} in the Pt/GC catalyst on its efficiency toward FAO. Initial results, although confirmed a dependence of the Pt/GC efficiency toward FAO on E_{Pt}, could not explore the origin of this enhancement [44]. In this study, the influence of E_{Pt} on the catalytic activity and, moreover, stability of the Pt/CC catalysts was deeply addressed. The electrochemical impedance spectroscopy (EIS) succeeded to understand the origin of enhancement of FAO at the different catalysts as a function of E_{Pt}.

2. EXPERIMENTAL

A glassy carbon (d = 6.0 mm) electrode served as the working electrode. A saturated calomel electrode (SCE: $Hg/Hg_2Cl_2/KCl$ (sat.)) and a spiral Pt wire were used as the reference and counter electrodes, respectively. All potentials in this investigation, even if not mentioned, were recorded in reference to this calomel electrode. Conventional procedure was applied to clean the GC electrode as described previously [45].

A fixed amount (applied charge, Q = 10 mC) of PtNPs was electrodeposited on the bare GC from 0.1 M H_2SO_4 + 1.0 mM $K_2[PtCl]_6$ solution via a constant potential technique. Based on the cyclic voltammogramm (CV) of the deposition of PtNPs, – 0.20, – 0.10, 0.00, 0.01 and 0.20 V were sought for the PtNPs potentiostatic deposition onto the GC electrode[44].

The electrochemical measurements were carried out in a traditional three-electrode glass cell at room temperature (~ 25 °C) using an EG&G potentiostat (model 273A) operated with Echem 270 software. The catalytic performance of the modified electrodes toward FAO was investigated in 0.3 M FA solution (pH = 3.5).

3. RESULTS AND DISCUSSION

The electrochemical characterization is a sensitive tool to assure the deposition of PtNPs at the GC surface. Figure 1 shows the characteristic CVs of the Pt/GC electrodes at which the PtNPswere electrodeposited at different potentials (E_{Pt}= – 0.20, – 0.10, 0.00, 0.10 and 0.20 V). The characteristic features of polycrystalline Pt were clearly observed in all catalysts. This involved the Pt oxidation which extended over a wide range of potentials (0.60 to 1.30 V) and the subsequent reduction of this oxide to Pt in the cathodic-going scan at ca. 0.35 V. In addition, the hydrogen adsorption/desorption ($H_{ads/des}$) peaks appeared in the potential range from 0.0 to – 0.2 V with intensities depended on E_{Pt}.We would like to highlight that the variation of these intensities or more precisely of the faradaic charges associated the $H_{ads/des}$ peaks inferred a correlative change in the real surface areas of PtNPs in the Pt/GC catalysts. This might result if PtNPs were deposited in different shapes or geometries. Table 1 shows the calculated Pt area (A_{Pt}) of the Pt/GC catalysts as a function of E_{Pt}. To be honest, Plyasova *et al*. have reported a key dependence of the structural defects and the lattice distortion of PtNPs in the Pt/GC catalyst on E_{Pt} that for sure affected the exposed surface area [46].

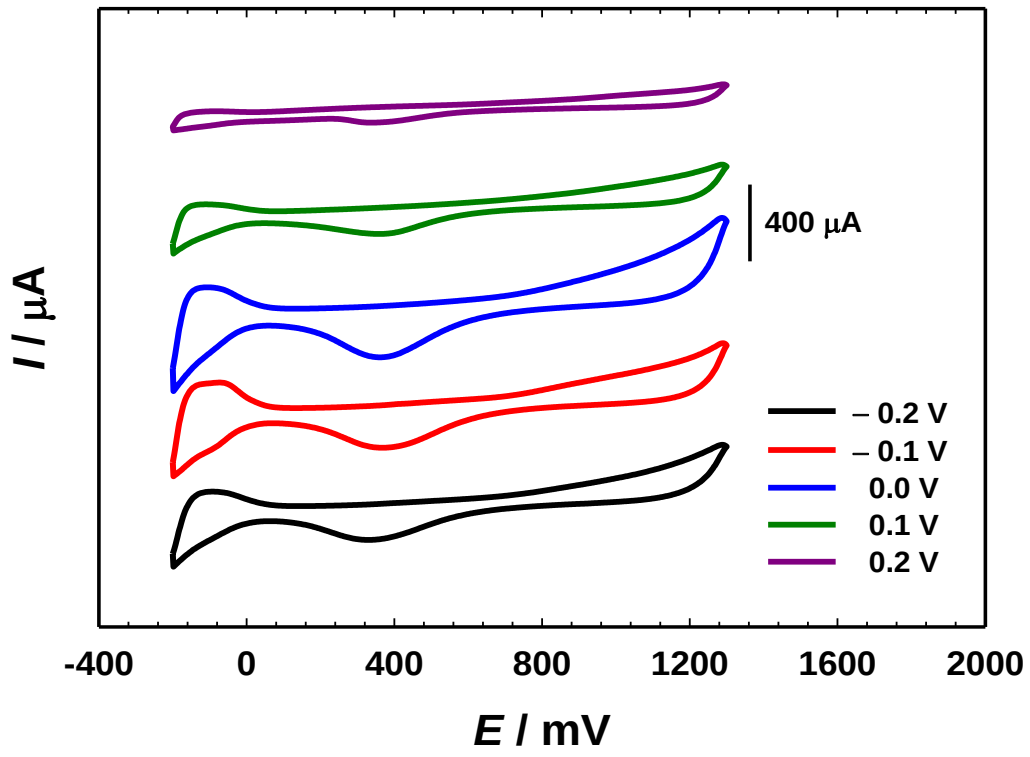

Figure 1. CVs obtained at the Pt/GC electrode in 0.1 M H_2SO_4 solution at different Pt electrodeposition potentials (E = – 0.20, – 0.10, 0.00, 0.10 and 0.20 V).

Table 1. The calculated Pt area (A_{Pt}) at differentE_{Pt}.

E_{Pt}/ V	A_{Pt} / cm^2
– 0.20	0.136
– 0.10	0.22
0.00	0.28
0.10	0.057
0.20	0.038

Figure 2 shows that the CVs of FAO at the Pt/GC catalysts in 0.3 M FA (pH = 3.5) solution at different E_{Pt} (– 0.20, – 0.10, 0.00, 0.10 and 0.20 V). Normally, at Pt-based catalysts, FAO takes place in two simultaneous pathways [47, 48]. The first is the dehydrogenation of FA to CO_2 (Eq. 1) at a low overpotential that makes the voltage output of DFAFCs closer to the theoretical value; hence, considered favorable. In Fig. 2, the peak observed at 0.3 V in the forward scan corresponded to this direct pathway and its peak current (I_p^d) inspired the density of the active "non-poisoned" Pt sites.

$$HCOOH(aq) + Pt \rightarrow Pt + CO_2(g) + 2H^+(aq) + 2e^- \quad (1)$$

The second pathway involves the *non-faradic* dissociation of FA at an open circuit potential to produce CO (Eq. 2) that gets adsorbed strongly at the Pt surface concealing many of the Pt active sites and blocking them from the participation in FAO.

$$HCOOH + Pt \rightarrow Pt\text{–}CO_{ads} + H_2O \quad (2)$$

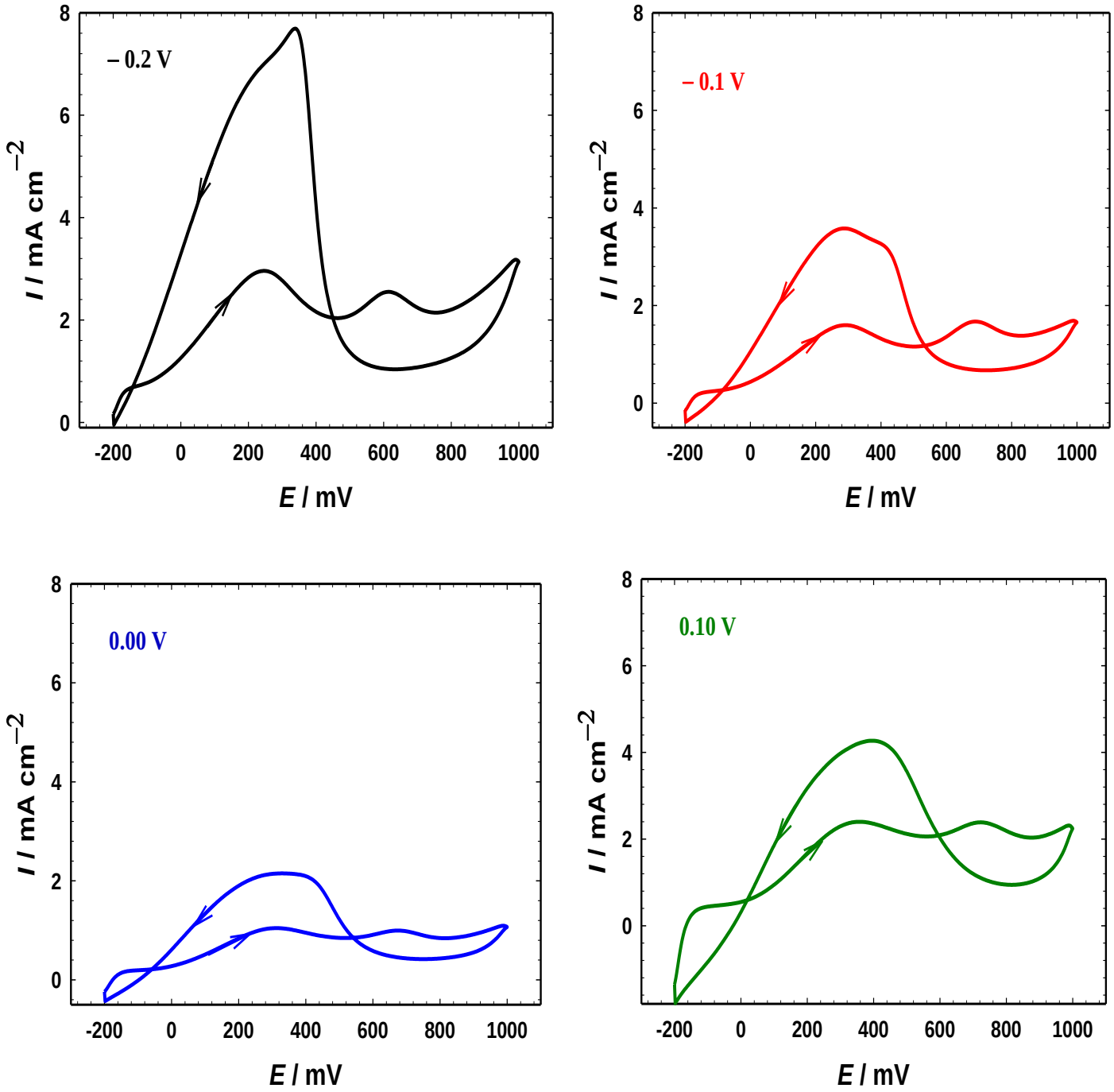

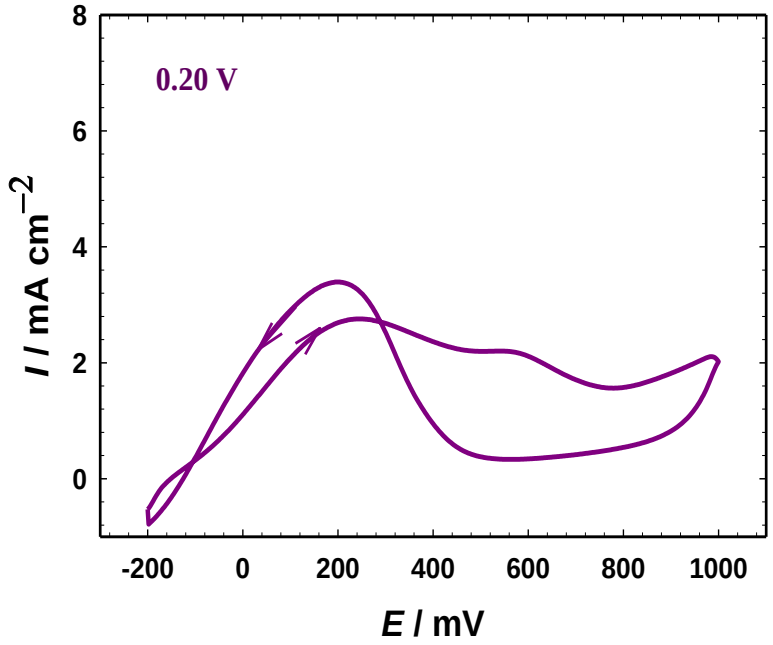

Figure 2. CVs of FAO at the Pt/GC catalysts in 0.3 M formic acid (pH = 3.5) solution at different E_{Pt} (– 0.20, – 0.10, 0.00, 0.10 and 0.20 V).

With biasing the overpotentials highly to the anodic direction, the Pt surface got hydroxylated to boost the oxidative CO removal indirectly at ca 0.6 V in the forward scan with a peak current (I_p^{ind}) that reflected the intensity of CO poisoning at the Pt surface. In the backward (cathodic-going) scan, after oxidizing most of the poisoning CO in the forward scan, FAO could proceed mainly via the direct pathway (see the peak at ca. 0.2 V in the backward cathodic scan and its corresponding peak current, I_p^b).

The I_p^d/I_p^{ind} and I_p^d/I_p^b ratios of all catalysts in Fig. 2 were utilized to compare the catalysts' activities toward FAO and their potential to mitigate the CO poisoning. Figure 3 and Table 2 shows that how the I_p^d, I_p^{ind}, I_p^b, I_p^d/I_p^{ind} and I_p^d/I_p^b changed with E_{Pt} for the prepared catalysts.

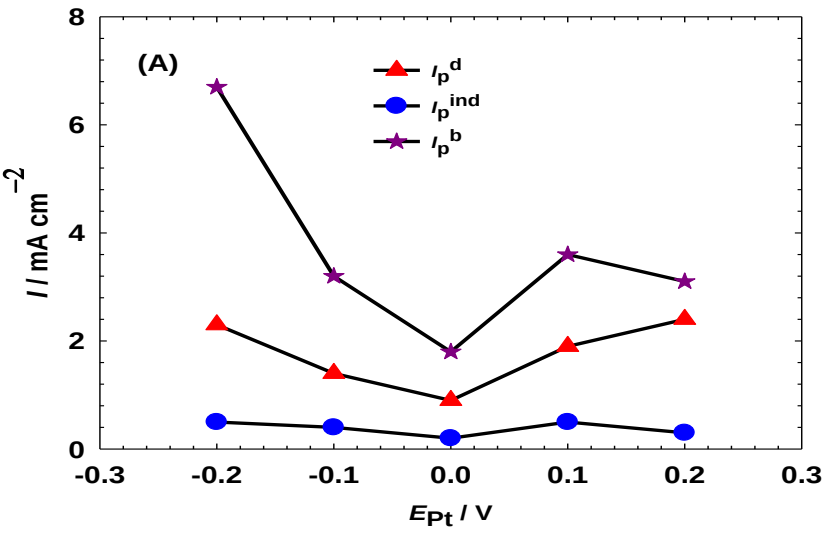

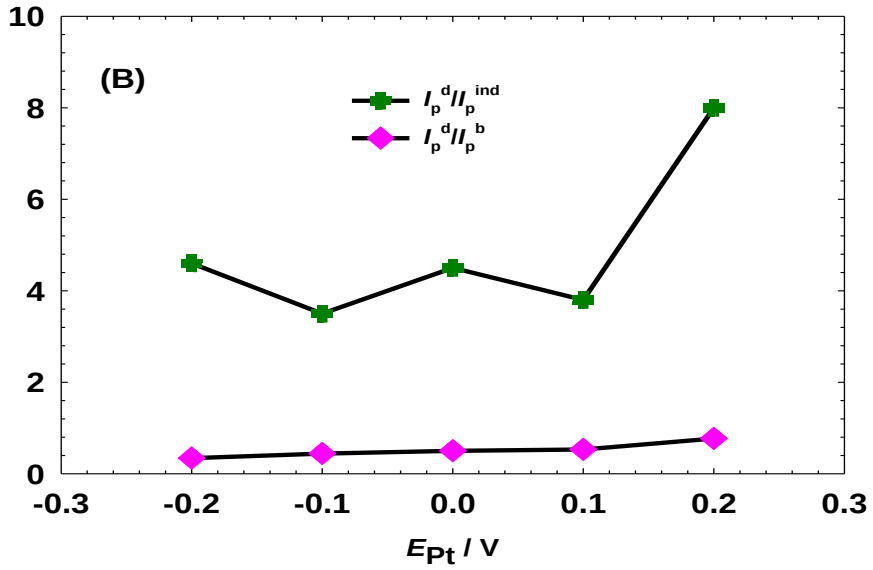

Figure 3. Dependence of the (A) I_p^d, I_p^{ind}, $I_p^b$and (B)I_p^d/I_p^{ind}, $I_p^d/I_p^b$of FAO at the Pt/GC catalysts on the E_{Pt}. Data were extracted from Fig. 2.

Table 2. Values of the I_p^d, I_p^{ind}, I_p^b, I_p^d/I_p^{ind} and $I_p^d/I_p^b$of FAO at the Pt/GC catalysts as a function of the E_{Pt}. Data were extracted from Fig. 2.

E_{Pt}/ V	I_p^d / $mAcm^{-2}$	I_p^{ind} / $mAcm^{-2}$	I_p^b / $mAcm^{-2}$	I_p^d/I_p^{ind}	I_p^d/I_p^b
– 0.20	2.3	0.5	6.7	4.6	0.3
– 0.10	1.4	0.4	3.2	3.5	0.44
0.00	0.9	0.2	1.8	4.5	0.50
0.10	1.9	0.5	3.6	3.8	0.53
0.20	2.4	0.3	3.1	8.0	0.77

As Fig. 3 and Table 2 show, the potentiostatic electrodeposition of PtNPs at fixed potentials (from – 0.20 to 0.2 V) exhibited catalytic activities much higher than both of the bare Pt and the Pt/GC (for which PtNPs were deposited by potential step electrolysis [24]) catalysts (See Tables 2 and 3). Careful evaluation of the results in Fig. 3 and Table 2 outlines the superiority of the Pt/GC catalyst (E_{Pt}= 0.2 V) for FAO where it achieved the highest I_p^d/I_p^{ind} (8.0) and I_p^d/I_p^b (0.77) ratios.The Pt/GC catalyst (E_{Pt}= –0.2 V) came the second in terms of its I_p^d/I_p^{ind} (4.6) ratio but its I_p^d/I_p^b (0.3) ratio was the worst. The Pt/GC catalyst (E_{Pt}= 0 V) was not so bad as it exhibited a high efficiency to steer the FAO in the direct pathway (I_p^d/I_p^{ind}= 4.5) and showed an intermediate tolerance against CO poisoning (I_p^d/I_p^b= 0.5). In fact, as mentioned previously, the variation in E_{Pt} in the Pt/GC is expected to develop important

morphological and/or structural changes in the catalyst. This would perhaps enrich the Pt surface in preferred orientations for FA adsorption (the essential step in the mechanism of FAO) and/or in the way weakening the Pt–CO bonding [38, 46, 49-53].We may not exclude the electronic contribution (easiness of charge transfer steps) association the structural modification of the Pt surface in the catalytic enhancement of the Pt/GC catalysts toward FAO. Luckily, the EIS could reveal important information about the charge transfer resistance (R_{ct}) of the catalyst toward FAO to assess the electronic contribution in their catalytic enhancement. Figure 4 that represents the Nyquist plots for all the Pt/GC catalysts in FA as functions of E_{Pt} could safely exclude the electronic contribution in the catalytic enhancement for the Pt/GC catalyst (E_{Pt}= 0.2 V) as it owned the highest R_{ct} (R_{ct} is determined from the diameter of the semicircle of the Nyquist plot). Interestingly, the R_{ct} of the Pt/GC catalysts increased in an obvious trend with the increase of E_{Pt} which highlighted the descending electronic contribution in the catalytic enhancement of the Pt/GC catalysts toward FAO. If the geometric contribution in the catalytic enhancement of FAO moved parallel (decreased with E_{Pt}) with the electronic contribution, one might expect the superiority of the Pt/GC catalyst (E_{Pt}= –0.2 V) toward FAO, which did not happen. It seems that with varying E_{Pt}, the trends of the geometric and electronic influences of the Pt/GC catalysts in the catalytic enhancement of FAO moved in opposite directions which resulted the catalytic behavior observed in Fig. 3 and Table 2.

Table 3. A comparison for the current and previous I_p^d/I_p^{ind} and I_p^d/I_p^b ratios obtained for FAO.

E_{Pt} / V	Catalyst	I_p^d / I_p^{ind}	I_p^d / I_p^b	*Ref.*
Potential step electrolysis from 1 to 0.1 V	Pt/GC	0.45–2	0.20–0.29	[24, 54]
Bare Polycrystalline Pt electrode	Pt	2.3	0.31	[55]
Bare Pt substrate	Pt	0.6	0.2	[56]
Potentiostatic at – 0.2 V(9.4 mC)	Pt/GC	0.76	0.39	[21]
Potentiostatic at 0.2 V(10 mC)	Pt/GC	8.0	0.77	This work

From another perspective, the good catalyst must acquire not only a good catalytic activity but also long-termed stability during the continuous electrolysis. Fig. 5 shows the chronoamperometric (*i*-*t*) curves measured for the Pt/GC catalysts prepared at different E_{Pt} in a continuous electrolysis in FA at a constant potential of 0.1 V. Actually, the Pt/GC catalysts (E_{Pt}= – 0.20, – 0.10, 0.10 and 0.20 V) catalysts displayed moderate stabilities over 30 min of continuous electrolysis in FA. The decay in the current density was most likely developed with a consequent structural/electronic modification in the Pt

surface which supported the CO poisoning. Remarkably, the Pt/GC catalyst (E_{Pt}= 0.00 V) exhibited the highest stability toward the continuous electrolysis in FA with the lowest decay in the current density. Owing to its moderate activity (see Table 2), the Pt/GC catalyst (E_{Pt}= 0.00 V) would be a good choice for FAO. As we just mentioned, there was a competition between the geometric and electronic enhancement of the catalysts toward FAO with the variation of E_{Pt} which might carry the responsibility of the high durability of the Pt/GC catalyst (E_{Pt}= 0.00 V) which was subjected to a further geometrical/electronic change with the continuous electrolysis. Table 4 summarizes the decay percentage of the current density of FAO for all the prepared Pt/GC catalysts.

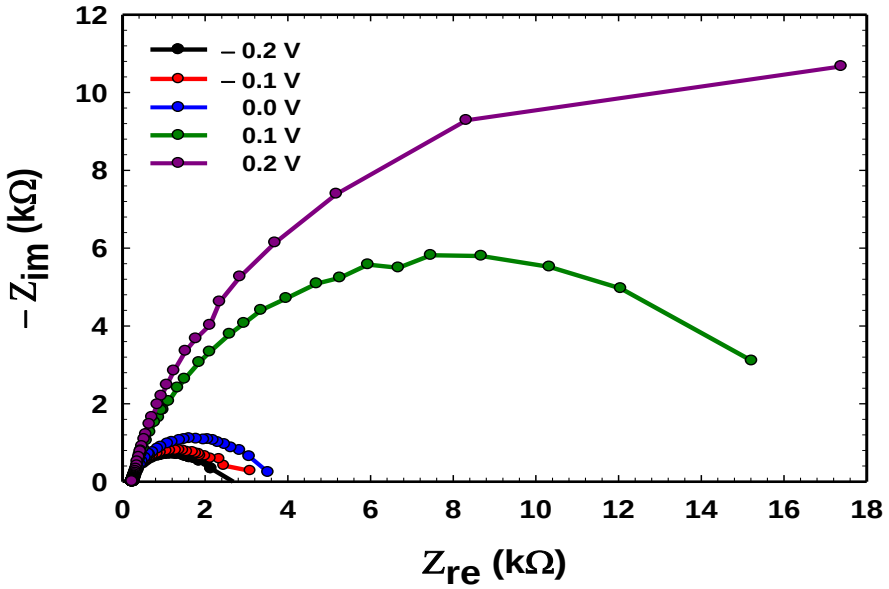

Figure 4. Nyquist plots measured at 0.3 V in 0.3 M HCOOH (pH 3.5) for the Pt/GC catalysts at different E_{Pt} (– 0.20, – 0.10, 0.00, 0.10 and 0.20 V).

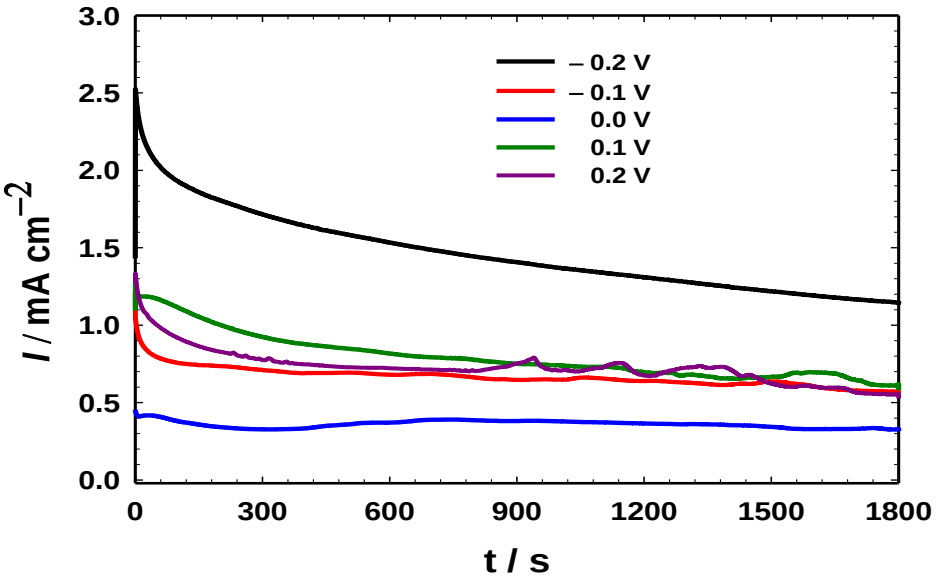

Figure 5. Chronoamperometric (*i*-*t*) curves measured at 0.1 V in 0.3 M HCOOH (pH 3.5) for the Pt/GC catalysts at different E_{Pt} (– 0.20, – 0.10, 0.00, 0.10 and 0.20 V).

Table 4. The decay percentage of the current density of FAO for all prepared Pt/GC catalysts at different E_{Pt}(– 0.20, – 0.10, 0.00, 0.10 and 0.20 V).

E_{Pt}/ V	*Decay %*
– 0.20	46
– 0.10	44
0.00	26
0.10	49
0.20	46

4. CONCLUSION

The Pt deposition onto the GC electrode was carried out by a potentiostatic technique at different potentials, E_{Pt}. Electrochemical investigations confirmed that the Pt/GC catalyst at which PtNPs were deposited at E_{Pt}=0.20 V acquired the highest catalytic activity (I_p^d/I_p^{ind}= 8) toward FAO and the best tolerance against CO poisoning (I_p^d/I_p^b= 0.77). The catalytic enhancement of this catalyst (Pt/GC (E_{Pt}= 0.20 V)) toward FAO was originated principally from geometric/structural concerns as this catalyst owned the highest charge transfer resistance. On the other hand, the Pt/GC catalyst (E_{Pt}= 0.00 V) displayed the highest durability toward FAO with the lowest decay (26 %) in the current density in a continuous electrolysis in FA for 30 min. This investigation highlighted the importance of optimizing the deposition conditions of Pt catalysts in DFAFCs even before amendment with further modifiers.

ACKNOWLEDGEMENT
This research was supported from the General Scientific Research Department of Cairo University, Egypt (Grant 77/2016).

References

1. A. Boddien, D. Mellmann, F. Gärtner, R. Jackstell, H. Junge, P. J. Dyson, G. Laurenczy, R. Ludwig, M. Beller, *Science*, 333 (2011) 1733.
2. C. Li, Q. Yuan, B. Ni, T. He, S. Zhang, Y. Long, L. Gu, X. Wang, *Nat. Commun.*, 9 (2018) 3702.
3. I. M. Al-Akraa, A. M. Mohammad, M. S. El-Deab, B. S. El-Anadouli, *Int. J. Electrochem. Sci.*, 10 (2015) 3282.
4. I. M. Al-Akraa, *Int. J. Hydrogen Energy*, 42 (2017) 4660.
5. F. Xia, S. E. C. Dale, R. A. Webster, M. Pan, S. Mu, S. C. Tsang, J. M. Mitchels, F. Marken, *New J. Chem.*, 35 (2011) 1855.
6. N. Cheng, H. Lv, W. Wang, S. Mu, M. Pan, F. Marken, *J. Power Sources*, 195 (2010) 7246.
7. N. Cheng, R. A. Webster, M. Pan, S. Mu, L. Rassaei, S. C. Tsang, F. Marken, *Electrochim. Acta*, 55 (2010) 6601.
8. I. M. Al-Akraa, T. Ohsaka, A. M. Mohammad, *Arab. J. Chem.*, 12 (2019) 897.

9. I. M. Al-Akraa, A. M. Mohammad, M. S. El-Deab, B. E. El-Anadouli, *Arab. J. Chem.*, 10 (2017) 877.
10. M. K. Debe, *Nature*, 486 (2012) 43.
11. Y. Wang, K. S. Chen, J. Mishler, S. C. Cho, X. C. Adroher, *Appl. Energy*, 88 (2011) 981.
12. R. Borup, J. Meyers, B. Pivovar, Y. S. Kim, R. Mukundan, N. Garland, D. Myers, M. Wilson, F. Garzon, D. Wood, P. Zelenay, K. More, K. Stroh, T. Zawodzinski, J. Boncella, J. E. McGrath, M. Inaba, K. Miyatake, M. Hori, K. Ota, Z. Ogumi, S. Miyata, A. Nishikata, Z. Siroma, Y. Uchimoto, K. Yasuda, K. I. Kimijima, N. Iwashita, *Chem. Rev.*, 107 (2007) 3904.
13. B. C. H. Steele, A. Heinzel, *Nature*, 414 (2001) 345.
14. G. A. El-Nagar, A. M. Mohammad, M. S. El-Deab, B. E. El-Anadouli, in *Progress in Clean Energy, Volume 1: Analysis and Modeling*. (Springer International Publishing, 2015), pp. 577-594.
15. S. M. El-Refaei, G. A. El-Nagar, A. M. Mohammad, B. E. El-Anadouli, in *Progress in Clean Energy, Volume 1: Analysis and Modeling*. (Springer International Publishing, 2015), pp. 595-604.
16. N. M. Aslam, M. S. Masdar, S. K. Kamarudin, W. R. W. Daud, *APCBEE Procedia*, 3 (2012) 33.
17. Y.-W. Rhee, S. Y. Ha, R. I. Masel, *J. Power Sources*, 117 (2003) 35.
18. X. Wang, J.-M. Hu, I. M. Hsing, *J. Electroanalytical Chemistry*, 562 (2004) 73.
19. U. B. Demirci, *J. Power Sources*, 169 (2007) 239.
20. X. Yu, P. G. Pickup, *J. Power Sources*, 182 (2008) 124.
21. Y. M. Asal, I. M. Al-Akraa, A. M. Mohammad, M. S. El-Deab, *Int. J. Hydrogen Energy*, 44 (2019) 3615.
22. Y. M. Asal, I. M. Al-Akraa, A. M. Mohammad, M. S. El-Deab, *J. Taiwan Inst. Chem. Eng.*, 96 (2019) 169.
23. I. M. Al-Akraa, Y. M. Asal, A. M. Mohammad, *J. Nanomater.* , 2019 (Article ID 2784708) (2019): https://doi.org/10.1155/2019/2784708.
24. A. M. Mohammad, I. M. Al-Akraa, M. S. El-Deab, *Int. J. Hydrogen Energy*, 43 (2018) 139.
25. I. M. Al-Akraa, A. M. Mohammad, M. S. El-Deab, B. E. El-Anadouli, *J. Electrochem. Soc.*, 162 (2015) F1114.
26. H. Lee, S. E. Habas, G. A. Somorjai, P. Yang, *J. Am. Chem. Soc.*, 130 (2008) 5406.
27. S. Y. Uhm, S. T. Chung, J. Y. Lee, *Electrochem. Commun.*, 9 (2007) 2027.
28. N. M. Markovic, H. A. Gasteiger, P. N. R. Jr., X. Jiang, I. Villegas, M. J. Weaver, *Electrochim. Acta*, 40 (1995) 91.
29. G. A. El-Nagar, A. M. Mohammad, M. S. El-Deab, T. Ohsaka, B. E. El-Anadouli, *J. Power Sources*, 265 (2014) 57.
30. A. M. Mohammad, S. Dey, K. K. Lew, J. M. Redwing, S. E. Mohney, *J. Electrochem. Soc.*, 150 (2003) G577.
31. A. M. Mohammad, T. A. Salah Eldin, M. A. Hassan, B. E. El-Anadouli, *Arab. J. Chem.*, 10 (2017) 683.
32. G. A. El-Nagar, M. S. El-Deab, A. M. Mohammad, B. E. El-Anadouli, *Electrochim. Acta*, 180 (2015) 268.
33. I. M. Sadiek, A. M. Mohammad, M. E. El-Shakre, M. S. El-Deab, B. E. El-Anadouli, *J. Solid State Electrochem.*, 17 (2013) 871.
34. I. M. Al-Akraa, A. M. Mohammad, M. S. El-Deab, B. E. El-Anadouli, *Int. J. Electrochem. Sci.*, 8 (2013) 458.
35. I. M. Al-Akraa, Y. M. Asal, A. M. Arafa, *Int. J. Electrochem. Sci.*, 13 (2018) 8775.
36. I. M. Al-Akraa, Y. M. Asal, S. D. Khamis, *Int. J. Electrochem. Sci.*, 13 (2018) 9712.
37. I. M. Al-Akraa, A. M. Mohammad, M. S. El-Deab, B. E. El-Anadouli, *Int. J. Hydrogen Energy*, 40 (2015) 1789.

38. I. M. Al-Akraa, A. M. Mohammad, M. S. El-Deab, B. S. El-Anadouli, *Int. J. Electrochem. Sci.*, 10 (2015) 3282.
39. I. M. Al-Akraa, A. M. Mohammad, M. S. El-Deab, B. E. El-Anadouli, *Int. J. Electrochem. Sci.*, 7 (2012) 3939.
40. S. M. Baik, J. Han, J. Kim, Y. Kwon, *Int. J. Hydrogen Energy*, 36 (2011) 14719.
41. C. Rice, S. Ha, R. I. Masel, A. Wieckowski, *J. Power Sources*, 115 (2003) 229.
42. W. S. Jung, J. Han, S. Ha, *J. Power Sources*, 173 (2007) 53.
43. S. D. Han, J. H. Choi, S. Y. Noh, K. Park, S.K.Yoon, Y. W. Rhee, *Korean J. Chem. Eng.*, 26 (2009) 1040.
44. I. M. Al-Akraa, B. A. Al-Qodami, A. M. Mohammad, *Int. J. Electrochem. Sci.*, 15 (2020) in press.
45. M. S. El-Deab, G. H. El-Nowihy, A. M. Mohammad, *Electrochim. Acta*, 165 (2015) 402.
46. L. M. Plyasova, I. Y. Molina, A. N. Gavrilov, S. V. Cherepanova, O. V. Cherstiouk, N. A. Rudina, E. R. Savinova, G. A. Tsirlina, *Electrochim. Acta*, 51 (2006) 4477.
47. R. Larsen, S. Ha, J. Zakzeski, R. I. Masel, *J. Power Sources*, 157 (2006) 78.
48. J. D. Lović, A. V. Tripković, S. L. J. Gojković, K. D. Popović, D. V. Tripković, P. Olszewski, A. Kowal, *J. Electroanal. Chem.*, 581 (2005) 294.
49. W. H. Qi, M. P. Wang, *J. Nanopart. Res.*, 7 (2005) 51.
50. M. Rezaei, S. H. Tabaian, D. F. Haghshenas, *Electrochim. Acta*, 59 (2012) 360.
51. P. Kalimuthu, S. A. John, *J. Electroanal. Chem.*, 617 (2008) 164.
52. N. Hoshi, M. Nakamura, K. Kida, *Electrochem. Commun.*, 9 (2007) 279.
53. L. Zhang, Q. Sui, T. Tang, Y. Chen, Y. Zhou, Y. Tang, T. Lu, *Electrochem. Commun.*, 32 (2013) 43.
54. M. S. El-Deab, G. A. El-Nagar, A. M. Mohammad, B. E. El-Anadouli, *J. Power Sources*, 286 (2015) 504.
55. B. A. Al-Qodami, H. H. Farrag, S. Y. Sayed, N. K. Allam, B. E. El-Anadouli, A. M. Mohammad, *J. Nanotechnol.*, 2018 (Article ID 4657040) (2018): https://doi.org/10.1155/2018/4657040.
56. I. M. Al-Akraa, A. M. Mohammad, *Arab. J. Chem.*, in Press (2019): https://doi.org/10.1016/j.arabjc.2019.10.013.